



Investigation of unaged and long-term aged bio-based asphalt mixtures containing lignin according to the VECD theory

Elena Gaudenzi · Lorenzo Paolo Ingrassia · Fabrizio Cardone · Xiaohu Lu · Francesco Canestrari

Received: 10 January 2023 / Accepted: 28 March 2023
© The Author(s) 2023

Abstract In the near future, the world of civil and building engineering will be dominated by the advent of bio-materials. Even the road paving sector is involved in the transition towards more sustainable solutions, promoting at the same time environmental benefits and economic savings. Currently, one of the main goals is to ensure that bio-binders offer good performance, at least comparable with that offered by conventional materials. In the last decades, the exponential increase in traffic volumes has led to various types of asphalt pavement distresses, among which fatigue cracking is one of the most common. Within this context, this study presents the characterization of a bio-based asphalt mixture obtained by replacing 30% of bitumen with lignin, which was compared with a reference asphalt mixture containing a plain bitumen characterised by the same penetration grade. Laboratory produced and compacted specimens were subjected to complex modulus and cyclic fatigue tests with the Asphalt Mixture Performance Tester (AMPT). Both unaged and long-term aging conditions were investigated. The tests and the subsequent

analyses were based on the simplified viscoelastic continuum damage (S-VECD) approach. Overall, the results showed that the presence of lignin led to a lower aging susceptibility, but also caused a slight reduction in fatigue life due to an increase in the material stiffness. Furthermore, the obtained results confirmed previous findings deriving from the study of the two binders and from the conventional characterization of the same asphalt mixtures as well.

Keywords Bio-binder · Lignin · Asphalt mixtures · Fatigue · Viscoelastic continuum damage (VECD) theory · Sustainability

1 Introduction

In the last decades, the use of bio-materials has gained notable interest in the civil engineering sector. In this context, the road industry is interested in developing new “green” solutions that concurrently meet the desired performance requirements of conventional materials. Given the rapid growth of cities and traffic volumes [1], the demand for raw materials for pavement construction and maintenance has dramatically increased, along with their price. At the same time, the environmental issues related to the carbon footprint and greenhouse gas emissions in the atmosphere due to the use of non-renewable resources cannot be neglected. For these reasons, bio-binders are

E. Gaudenzi (✉) · L. P. Ingrassia · F. Cardone · F. Canestrari
Department of Civil and Building Engineering and Architecture, Università Politecnica Delle Marche, Via Brecce Bianche, 60131 Ancona, Italy
e-mail: e.gaudenzi@pm.univpm.it

X. Lu
Nynas AB, 149 82 Nynäshamn, Sweden



currently considered a promising solution for flexible pavements. They consist in a partial or total replacement of bitumen, which derives from the distillation process of crude oil, with various bio-resources such as animal waste, bio-oils (wood, sunflower, corn, soybean) [2–4] waste cooking oil [5], and lignin [6–8]. In particular, lignin is gaining much interest since it is largely available in nature [9–11]. It can be in dusty or liquid form and derives from specific pyrolysis [12] or hydrolysis [13] processes carried out on wastes of the wood pulp and paper industries. From a structural point of view, it is a complex organic polymer with some chemical structures not dissimilar from bitumen. Indeed, they are both hydrocarbon materials mainly composed of carbon, hydrogen and oxygen [14, 15] and for this reason they might be compatible with each other. However, the main issue is to ensure that its application in asphalt mixtures does not produce negative effects or penalise the final performance.

Flexible pavements are affected by cyclic traffic loads, weathering and serious temperature fluctuations, which lead to several kinds of distresses and to the change of their mechanical properties (stiffness, permanent deformation resistance, fatigue resistance) over time. One of the major forms of distress is fatigue cracking, which causes a progressive reduction of the bearing capacity of the pavement. The development of the fatigue cracks occurs in the weakest component of the whole asphalt mixture system, i.e., in the binder phase [16]. If the failure occurs at the base of the asphalt layers, an upward cracking propagation takes place, which is called bottom-up cracking. It consists in a bending-induced phenomenon determined by the repeated passage of vehicles, which causes the onset of tensile stresses/strains at the bottom of the layer. Alternatively, another fatigue failure mechanism, called top-down cracking, can occur. It is mainly induced by the tire-pavement contact stresses, leading to the initiation of surface cracks that tend to propagate downwards [17]. Therefore, the fatigue cracking resistance of asphalt pavements is given by the design of the pavement structure in terms of layer thickness, type of materials, aggregate gradation, binder content, air voids content, etc., in relation to the design traffic loads.

In this regard, bio-binders and bio-mixtures, including lignin-based ones, have recently been investigated by several authors worldwide. At the binder level, it was mainly found that lignin slightly

reduces fatigue life as compared to conventional bitumen, regardless of its type/content and testing conditions [7, 8, 18–20], even though some investigations highlight an increase of fatigue life after aging [21]. This could be attributable to the stiffening effect usually produced by the presence of lignin [7, 11, 22], which could lead to a more brittle material but at the same time less susceptible to aging thanks to its antioxidant potential [11, 23, 24], thus resulting in a certain compensation of the effects. However, these results should be verified also at the mixture level, which is more correlated with the field performance of the pavement. Zhang et al. [25] evaluated the fatigue cracking resistance of asphalt mixtures by means of four-point bending tests. They found that, at a given strain level, asphalt mixtures containing 10% of powder lignin by weight of bitumen showed significant longer life than the reference mixture in unaged conditions. On the contrary, the asphalt mixture containing lignin fibres was less performing, and this unexpected result could be attributable to a possible poor compatibility between lignin fiber and bitumen, hence influencing the bonding with the aggregates. Gaudenzi et al. [26] examined the effects of powder lignin from two different sources dosed at 30% by weight of bitumen on the fatigue life of asphalt mixtures (both in unaged and long-term aged conditions) through indirect tensile tests. They found that both lignin-based asphalt mixtures showed a slightly penalised behaviour before aging compared to the reference mixture, whereas conflicting results appeared after long-term aging. In particular, one of the two mixtures containing lignin performed better than the reference one, while the other mixture performed worse than the reference one, leading to the assumption that the mixture behaviour was significantly influenced by the lignin type. Overall, non-univocal results were found in the literature on the fatigue performance offered by lignin-based asphalt binders and mixtures. The highlighted discrepancies could be due to the strong influence of the raw material from which lignin derives, its consistency (i.e., powder, liquid, fiber form) and replacement amount [6] and, above all, to the fact that the available results reflect the specific boundary conditions given by the tests performed [16, 27].

Indeed, the conventional testing methods for characterising the fatigue behaviour of asphalt mixtures do not allow to include simultaneously the effects of the



rate, mode and type of loading (stress/strain controlled, haversine or sinusoidal), rest periods, temperature, etc. [28]. In addition, stiffness, volumetric composition, geometry of the specimens (i.e., trapezoidal, prismatic, cylindrical) and testing configurations (i.e., uniaxial tension/compression, two/three/four-point bending, indirect tension, direct tension) strongly influence the response of the investigated material [29], leading to a fatigue characterization that is not fully realistic. For all these reasons, a great number of test repetitions is usually necessary, along with significant efforts and time for sample production, testing and analysis of the results [28]. Hence, the abovementioned aspects highlight the need to develop an alternative testing framework to investigate the fatigue behaviour of asphalt mixtures in a more reliable and quick way. In this regard, the simplified viscoelastic continuum damage (S-VECD) approach is gaining wide acceptance since it allows the prediction of the fatigue performance of asphalt mixtures under any temperature and loading conditions [30], which is very important for pavement design and management [31]. In fact, the main advantage of the S-VECD approach is that it allows to determine the intrinsic properties of the material, thus removing the dependence of the test results from the specific testing and boundary conditions while ensuring, at the same time, the reduction of the test repetitions. The viscoelastic continuum damage (VECD) theory was originally conceived for the characterization of conventional hot mix asphalt (HMA), but more recently it has been successfully applied also to warm recycled asphalt mixtures [32, 33], asphalt mixtures modified with waste plastic [34], and bio-asphalt mixtures containing bio-oil [35].

Within this context, this study focuses on the application of the S-VECD approach to compare the fatigue performance of an asphalt mixture containing lignin and a conventional asphalt mixture (selected as reference), both in unaged and long-term aged conditions. Binder phase analysis [36] and a conventional mechanical characterization [26, 37] have been previously conducted on the same materials. Thus, a correlation between the S-VECD findings and the previous results gathered from the conventional approach was also sought.

2 Background of VECD theory and S-VECD testing approach

The VECD model for the characterization of the fatigue performance of asphalt mixtures is founded on three main theoretical pillars:

1. The elastic–viscoelastic correspondence principle [38, 39]: it allows to replace the physical strains ε with the pseudo-strains ε^R , thus reducing the viscoelastic problem to the corresponding elastic problem. Therefore, viscous effects can be separated from damage-related effects, and time-dependence is overcome.
2. The continuum damage mechanics-based work potential theory [40]: the material is considered as a continuous and homogeneous body, and the damage growth caused by the microstructural deterioration can be modelled by directly evaluating the effects on the macroscopic behaviour.
3. The time–temperature superposition principle with growing damage [41]: it allows to consider the combined effect of time/rate of load application and temperature even outside the linear domain of the material behaviour.

The theoretical framework is based on the definition of pseudo-strain energy W^R by Schapery [38, 42]:

$$W^R = \frac{1}{2} E_R \cdot C(S) \cdot [\varepsilon^R(t)]^2 \quad (1)$$

where E_R is a constant reference modulus, typically taken as 1; $C(S)$ is the pseudo-stiffness, which represents the integrity of the material as a function of the internal state variable corresponding to the damage intensity S ; $\varepsilon^R(t)$ is the pseudo-strain time history.

The evolution of damage S is defined by a power law proposed by Park et al. [43]:

$$\frac{dS}{dt} = \left(-\frac{\partial W^R}{\partial S} \right)^\alpha \quad (2)$$

in which α is the damage growth rate that is related to the time-dependence of the relaxation modulus of the material in the linear viscoelastic domain. Specifically, all formulations above refer to the localised region of the macrocrack before damage coalescence, for which theoretical adjustments to the model would be required.

The relationship between pseudo-stiffness C and amount of damage S , known as damage characteristic relationship, can be expressed as in Eq. (3):

$$C = 1 - C_{11} \cdot S^{C_{12}} \quad (3)$$

where C_{11} and C_{12} are fitting coefficients. It is worth noting that the C vs S curve is a unique function describing the deterioration in material integrity as a result of damage accumulation [41]. Specifically, it is not dependent on testing conditions (temperature, frequency, stress–strain level) and loading control mode, but instead it represents the intrinsic property of the material to resist cracking, as long as viscous damping and microcrack damage can be considered the dominant energy-dissipating mechanisms [41, 44].

If cyclic loads are considered, the VECD model can be significantly simplified from the computational point of view and thus it is usually called S-VECD model [44]. In the S-VECD testing framework, the damage characteristic curve of a given asphalt mixture can be obtained by combining complex modulus and cyclic fatigue tests (performed in direct tension).

However, since the C vs S curve only defines the damage evolution within the material, it should always be combined with a fatigue failure criterion defining the material failure. For this purpose, Wang and Kim [45, 46] proposed the D^R criterion provided by Eq. (4).

$$D^R = \frac{\int_0^{N_f} (1 - C) dN}{N_f} = \frac{Cum(1 - C)}{N_f} \quad (4)$$

D^R is a material constant that is independent of mode of loading, temperature, stress/strain amplitude [47]. It represents the toughness of the material, i.e., the ability to absorb energy without fracturing, and is defined as the slope of the linear regression that passes through zero between the average reduction of the pseudo-stiffness up to failure, $Cum(1-C)$, and the number of cycles corresponding to failure, N_f . In particular, N_f corresponds to the cycle in which the product of the peak-to-peak stress and cycle number reaches a maximum value after a stable increase during cyclic loading [48].

Finally, a synthetic index quantifies the fatigue resistance of the asphalt mixture by combining stiffness, damage characteristics and toughness [48]:

$$s_{app} = 1000^{\left(\frac{\alpha}{2}-1\right)} \cdot \frac{a_T(S_{app})^{\frac{1}{\alpha+1}} \cdot \left(\frac{D^R}{C_{11}}\right)^{\frac{1}{C_{12}}}}{|E^*|_{LVE,S_{app}}^{\frac{\alpha}{4}}} \quad (5)$$

where α is the damage growth rate; $a_T(S_{app})$ is the time–temperature shift factor between the S_{app} temperature and the reference temperature considered for the complex modulus master curve; $|E^*|_{LVE,S_{app}}^{\frac{\alpha}{4}}$ is the reference modulus calculated at the S_{app} temperature and at the reduced frequency of $62.8 \cdot a_T(S_{app})$. Specifically, the S_{app} index refers to the average temperature of the climatic PG of the location where the pavement is constructed, minus 3 °C. The S_{app} values usually vary within a range of 0 to 50, and higher values indicate better fatigue resistance [33, 49].

Overall, the S-VECD testing approach can be acknowledged as a more advanced approach as compared to the conventional mechanical characterization tests, since it has a solid theoretical background and allows to determine the intrinsic properties of the material, which are independent of the boundary and loading conditions.

3 Materials and methods

3.1 Materials

A conventional reference asphalt mixture, coded as M50/70, and a bio-based asphalt mixture produced by using a lignin-based bitumen, coded as M70/100_S30, were designed according to the Italian technical specifications for binder courses [50]. The selected powder lignin of Swedish origin derives from thermochemical and enzymatic treatments of wood, and it was dosed at 30% by weight of binder to maximise the replacement of the base 70/100 pen. grade bitumen. For the preparation of the bio-binder, a standardized blending procedure was adopted. The 70/100 base bitumen was heated in a forced-draft oven for one hour at the blending temperature of 180 °C. Concurrently, lignin was finely crumbled and dried at 105 °C to remove all moisture. Then, dried lignin was added gradually to the base bitumen and dispersed through a high shear stirring mixer at a speed of 5000 rpm for about 30 min to obtain a homogenous bituminous blend. The bio-binder was properly designed in order

to have a similar consistency to that of the plain 50/70 pen grade bitumen commonly employed at Italian latitudes and used to produce the reference mixture M50/70. The characteristics of the reference bitumen and the lignin-based binder are listed in Table 1 [37].

Both mixtures, M50/70 and M70/100_S30, were characterised by the same aggregate gradation, obtained by combining different fractions of limestone aggregates and 15% of reclaimed asphalt pavement (RAP) (Table 2), analogously to previous laboratory experience [26]. The nominal maximum aggregate size (NMAS) was equal to 16 mm.

The two mixtures differed for the binder content, which was optimised based on volumetric considerations, as described by Gaudenzi et al. [37]. As a result of such optimisation, a bitumen content equal to 5.4% was adopted for the reference mixture M50/70, whereas a bio-binder content of 6.4% (corresponding to 4.6% of total bitumen plus 1.8% of lignin) was used to produce the lignin-based asphalt mixture M70/100_S30, with a consequent bitumen saving of 15%. More details about the lignin and lignin-based binder can be found in [36].

3.2 Preparation of the specimens

The reference asphalt mixture M50/70 was mixed and compacted at the respective temperatures of 150 °C and 138 °C, while higher temperatures equal to 180 °C and 167 °C were adopted for the lignin-based asphalt mixture M70/100_S30, thus ensuring equi-viscosity conditions in accordance with NCHRP 648 specifications [51]. After the mixing phase, the loose asphalt mixtures were subjected to short-term aging in a forced-draft oven at 135 °C for 4 h, according to the protocol reported in the standard AASHTO R 30 [52]. Then, cylindrical samples with a diameter of 150 mm and a height of 180 mm were produced with a gyratory compactor. Since this condition corresponds to the actual state of the mixture at the beginning of its

Table 1 Characteristics of the reference bitumen and the bio-binder

Binder	Penetration (0.1 mm)	Softening point (°C)
50/70	52	51.6
70/100_S30	58	48.8

Table 2 Aggregate fractions used to produce the investigated mixtures

Aggregate fraction (mm)	10/16	6/12	0/4	filler	RAP
Percentage (%)	20	22	37	6	15

service life, it was referred to as the “unaged” condition in this experimental investigation. From each gyratory sample, 4 test specimens with 38 mm diameter and 110 mm height were obtained by coring and cutting the specimen according to the standard AASHTO PP 99 [53]. The reduced geometry of the specimen allows to save conditioning and testing time as well as the amount of material needed, and it is considered representative for dense-graded mixtures characterised by NMAS lower than 19 mm. In addition, part of the 38 mm test specimens were long-term aged in the oven at 85 °C for 5 days, according to the protocol by AASHTO R 30 [52]. The target air void content of the test specimens, assessed according to EN 12,697–6 – Procedure A: Bulk density (dry method) [54], was chosen as $5 \pm 0.5\%$. Specimens which did not fall within the abovementioned range of air voids were rejected (i.e., not tested).

3.3 Complex modulus tests

Complex modulus tests were carried out on 38 mm diameter specimens in accordance with AASHTO TP 132 [55] by means of the Asphalt Mixture Performance Tester (AMPT). The samples were subjected to sinusoidal axial compression loading, with a controlled strain amplitude between 50 and 75 microstrain. Measurements were taken along three different verticals through LVDTs, which were placed in the central part of the specimen, 120° apart from each other. The complex modulus $|E^*|$ and the phase angle δ were recorded at six frequencies (0.1, 0.5, 1, 5, 10, 20 Hz) and four temperatures (4, 20, 40, 60 °C), except for the mixture M50/70 in unaged conditions, which was tested only at 4, 20 and 40 °C. At least three replicates for each asphalt mixture and aging condition were considered.

The experimental data obtained in terms of storage modulus ($E_1 = |E^*| \bullet \cos\delta$) were shifted through the time–temperature shift factors (Eq. (6)) at the reference temperature of 21.1 °C and then modelled



through the 2S2PID model (Eq. (7)), which is the combination of physical elements (two springs, two parabolic elements and one dashpot).

$$\log a_T = a_1 \cdot T^2 + a_2 \cdot T + a_3 \quad (6)$$

where a_1 , a_2 , a_3 are fitting coefficients, and T is the testing temperature.

$$E_1(i\omega\tau) = E_{1,0} + \frac{E_{1,\infty} - E_{1,0}}{1 + \zeta(i\omega\tau)^{-k} + (i\omega\tau)^{-h} + (i\omega\beta\tau)^{-1}} \quad (7)$$

where $E_{1,0}$ and $E_{1,\infty}$ are the storage modulus values for frequency $\omega \rightarrow 0$ and $\omega \rightarrow \infty$ respectively, representing the behaviour of the springs; k and h represent the two parabolic creep elements and their value ranges between 0 and 1; ζ is a proportional constant between the parabolic elements; β is a dimensionless parameter linked to the Newtonian viscosity of the dashpot [56].

The values of the 2S2PID parameters and the shift factors were determined simultaneously by minimising the error in terms of E_I .

3.4 Cyclic fatigue tests

Uniaxial cyclic fatigue tests were performed by means of the AMPT apparatus following the standard AASHTO TP 133 [48]. The test setup includes a couple of steel end plates to which the specimen is glued to eliminate any eccentricity, and three pairs of mounting studs glued to the specimen to allocate three LVDTs in the central part of the specimen and 120° apart from each other. The test is conducted at the selected frequency of 10 Hz and a constant temperature corresponding to the average of the binder PG minus 3 °C (not exceeding 21 °C). Since the PG of the reference bitumen and the lignin-extended binder was respectively equal to 64–16 and 76–22 [36], a testing temperature of 21 °C was selected for both mixtures (M50/70 and M70/100_S30) and aging conditions (unaged and long-term aged).

The procedure includes first the application of a low peak-to-peak strain magnitude (50–75 microstrain) to obtain the complex modulus fingerprint of the specimen in tension–compression mode of loading. The determination of the complex modulus during the fingerprint allows to limit the specimen-to-specimen variability and calibrate the target strain amplitude of

the subsequent fatigue test carried out on the specimen. In particular, the Dynamic Modulus Ratio (DMR) can be evaluated as the ratio between the fingerprint modulus value $|E^*|_{fingerprint}$ and the reference modulus value deriving from the master curve at the same temperature and frequency conditions. The value should be between 0.85 and 1.15 for the specimen to be considered representative. Then, direct tension cyclic fatigue tests were run. The fatigue tests were conducted in controlled actuator displacement, and the amplitude of the sinusoidal strain was set between 160 and 250 microstrain to obtain test durations (N_f) between 2000 and 80,000 cycles, in accordance with AASHTO TP 133 [48]. According to the reference standard, the test is considered valid only if a middle failure occurs (i.e., the failure surface should be entirely included in the measurement area). Moreover, at least three valid repetitions must be achieved for each mixture, considering different strain levels (i.e., different test durations).

The test data collected were then analysed according to the VECD theory, by using the dedicated spreadsheet FlexMAT™ Cracking (v.2.1.1) developed at North Carolina State University.

4 Results and analysis

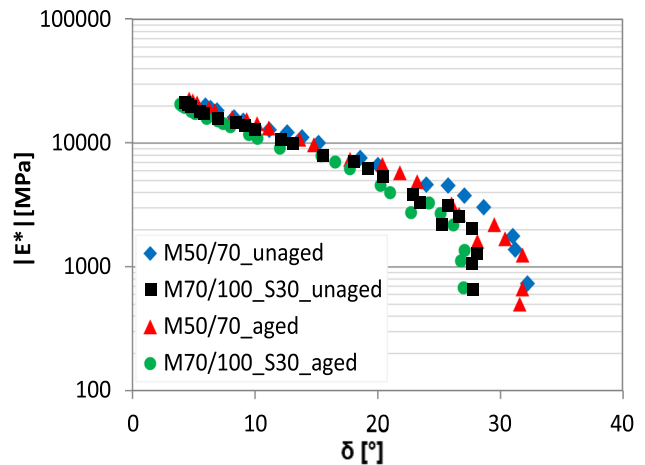
4.1 Complex modulus

The raw results deriving from the complex modulus tests were directly plotted in the Black diagram, i.e., the norm of the complex modulus $|E^*|$ as a function of the phase angle δ (Fig. 1). This representation does not require any manipulation of the rheological data and does not present any explicit information on the test temperature and frequency [57, 58].

The Black curves of all the investigated mixtures are smooth, suggesting the applicability of the Time–Temperature Superposition Principle [41]. A shift of the curves towards the upper left part of the graph is observed for the bio-asphalt mixtures, which is caused by the dual effect of the increase of complex modulus and decrease of phase angle. The first aspect suggests a stiffening effect due to lignin, whereas the second aspect indicates an enhanced elastic response. Moreover, as expected, a slight shift of the Black curve towards higher moduli and lower phase angles can be observed for both mixtures after long-term aging.



Fig. 1 Complex modulus results: Black diagram



The storage modulus master curves and phase angle master curves at the reference temperature of 21.1 °C are shown in Fig. 2a and b), respectively. All master curves were obtained by applying the shift factors determined from the minimisation of the error related to E_I (see Sect. 3.3). As already observed in Fig. 1, a higher stiffness of the mixture containing lignin can be noted, especially in the low frequency (i.e., high temperature) domain, while the master curves tend to converge at high frequency (i.e., low temperature). At the same time, lower phase angles are found for M70/100_S30 throughout the entire investigated frequency domain (Fig. 2b), which is indicative of a more pronounced elastic behaviour, but the gap between the materials tends to be minimised at high frequency. After long-term aging, as expected, an increase in E_I emerges for both materials, which is particularly notable in the low frequency (i.e., high temperature)

region. Moreover, the aging effects result in a shift towards lower values of phase angle. Overall, it seems that the reference mixture M50/70 is more sensitive to the aging effects as compared to the lignin-based mixture, especially at intermediate and low frequencies (intermediate and high temperatures). In this regard, the area below the log (reduced frequency)-log (E_I) curve, ranging between $1.59 \cdot 10^{-5}$ and $1.59 \cdot 10^5$, was determined by using the trapezoidal method in order to quantify the aging susceptibility of the investigated mixtures. The results, summarized in Table 3, confirm the lower aging susceptibility of the mixture containing lignin, as demonstrated by the percentage increase of E_I after aging ($\Delta = 7.3\%$ for M50/70 vs. 1.8% for M70/100_S30). This preliminary finding could be attributable to the recognised antioxidant properties of lignin [18, 59, 60], to the lower

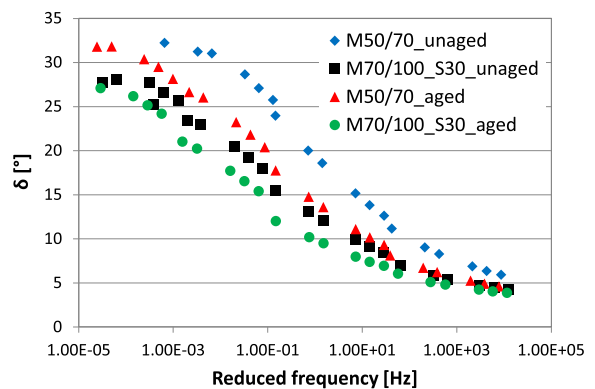
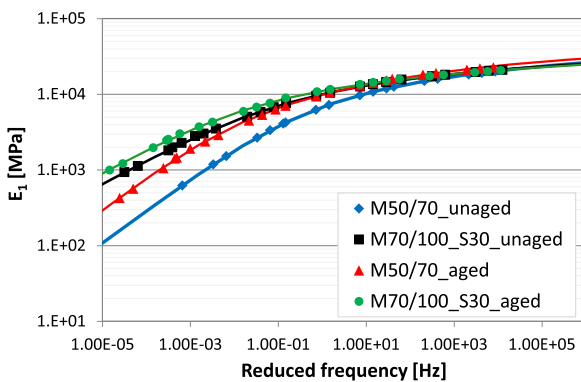


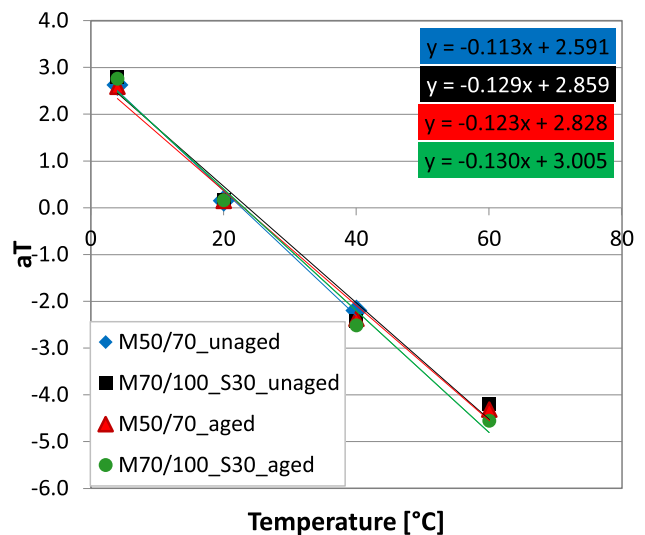
Fig. 2 Complex modulus results: **a** storage modulus master curves (experimental data and 2S2PID model) and **b** phase angle master curves at 21.1 °C

Table 3 Area below the master curves ($\log(\text{reduced frequency})-\log(E_f)$)

Mixture	Area	$\Delta_{\text{unaged/aged}}$
M50/70_unaged	50.38	7.3%
M50/70_aged	54.04	
M70/100_S30_aged	56.62	1.8%
M70/100_S30_unaged	57.64	

content of effective bitumen in the presence of lignin [37] or to a combination of both effects.

In addition, Fig. 3 presents the shift factor values, which are representative of the temperature-dependency of the mixtures studied. The fitting functions are broadly characterized by similar slope values regardless of the binder type and aging condition considered, denoting a similar thermal susceptibility. Specifically, slightly higher slopes are observed for the lignin-containing mixture than for the reference one under both aging conditions, denoting a slightly higher thermal susceptibility. Moreover, the expected reduced aging susceptibility of M70/100_S30 with respect to the reference mixture is confirmed by the lower variation of the slope of the fitting function after aging.

Fig. 3 Complex modulus results: shift factors

4.2 Fatigue behaviour

As an example of the raw fatigue data, Fig. 4 shows the evolution of the complex modulus and the product of stress and cycle number (whose maximum value defines N_f) during the fatigue test for a representative specimen of each asphalt mixture in long-term aged conditions. Despite both specimens refer to the same strain level (170 microstrain), the difference between them is evident. In fact, the fatigue resistance of the lignin-based asphalt mixture (M70/100_S30_aged) is lower than the conventional asphalt mixture (M50/70_aged), as highlighted by a faster loss of stiffness (Fig. 4a) and ultimately by a shorter fatigue life N_f (Fig. 4b).

As for the data analysed according to the VECD theory, the pseudo-stiffness C and the damage accumulation S up to failure are plotted against each other in Fig. 5. Specifically, Fig. 5a) shows the damage characteristic curves for individual specimens, while the representative fitting of each mixture is plotted in Fig. 5b) together with the corresponding fitting coefficients. The overlapped experimental curves in Fig. 5a) demonstrate the repeatability of the tests, which were conducted on selected specimens characterised by similar air voids (i.e., $5 \pm 0.5\%$). From the comparison between the reference and bio-based asphalt mixtures before aging, similar C values at failure can be noted, but the mixture containing lignin exhibits a greater S value at failure, which suggests that it may be characterized by better damage

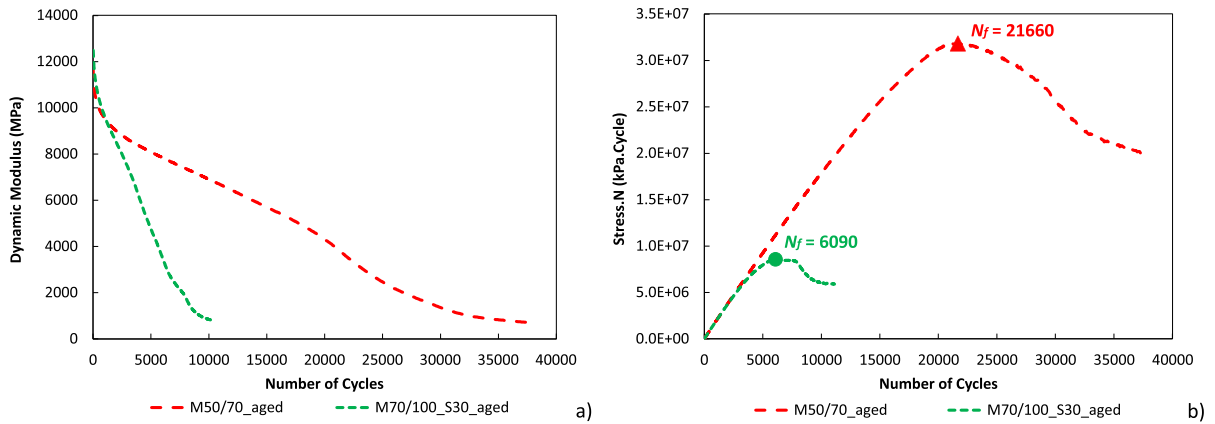


Fig. 4 Evolution of **a** complex modulus and **b** product of stress and cycle number during the fatigue test for two representative long-term aged specimens

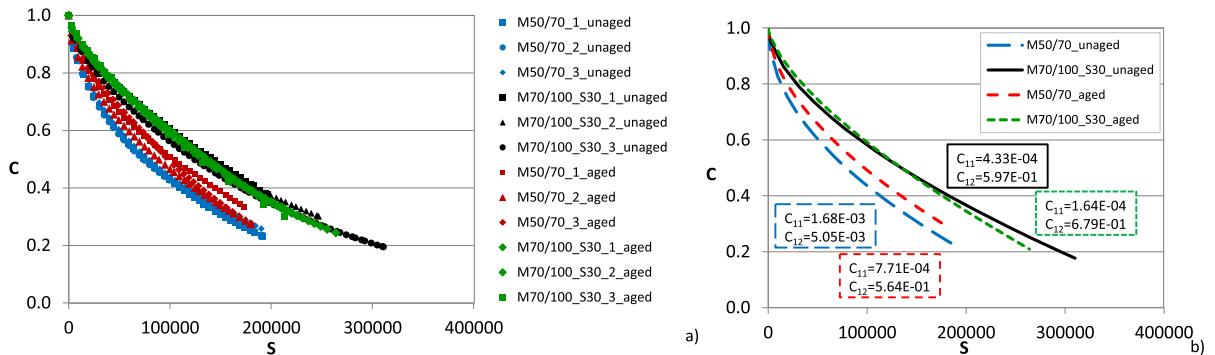


Fig. 5 Damage characteristic curves: **a** individual specimens, **b** power function fit for each asphalt mixture

tolerance and postponed failure, despite its higher stiffness (which is denoted by the upper position of its damage characteristic curve). If the reference mixture M50/70 is observed, aging causes a shift of the C vs S curve towards the higher part of the graph. This finding is attributable to the stiffness increase already observed from the complex modulus tests, which leads to higher pseudo-stiffness values up to failure, denoting a worsening of the damage tolerance capability of the mixture. This is a typical result for conventional asphalt mixtures, as already shown by previous investigations [61, 62]. Conversely, a different behaviour can be observed for the bio-based mixture, which shows longer damage characteristic curves (higher S values) and almost overlapped curves at both aging conditions, confirming its lower aging susceptibility. Moreover, an unexpected inversion of the curves related to the unaged and long-term aged conditions can also be observed for medium-high

damage levels. As a consequence, even after long-term aging, the lignin-based mixture shows a lower C value and a higher S value at failure with respect to the reference mixture, which would suggest higher tolerance to damage and postponed fatigue failure. Based only on the C vs S curves, it may appear that the investigated lignin-based mixture shows better fatigue behaviour with respect to the reference asphalt mixture. However, it is worth noting that the C vs S curves alone are not sufficient to fully interpret the fatigue behaviour of the mixtures. For this reason, they should always be combined with the corresponding D^R values (a measure of the material toughness) and used to calculate the S_{app} parameter (representative of the fatigue performance of the material within the pavement).

The relationships between the cumulative $(1-C)$ up to failure and the number of loading cycles at failure are plotted in Fig. 6. The slope of such relationships is



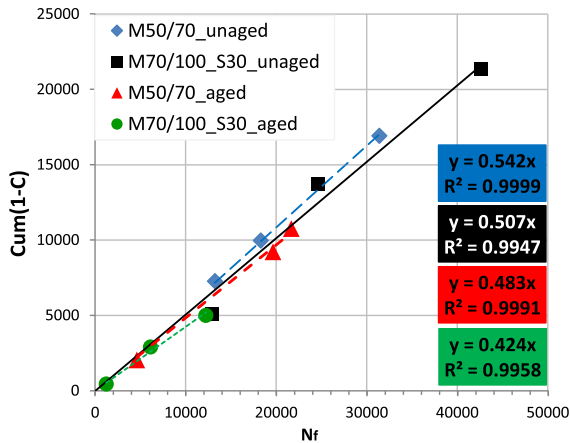
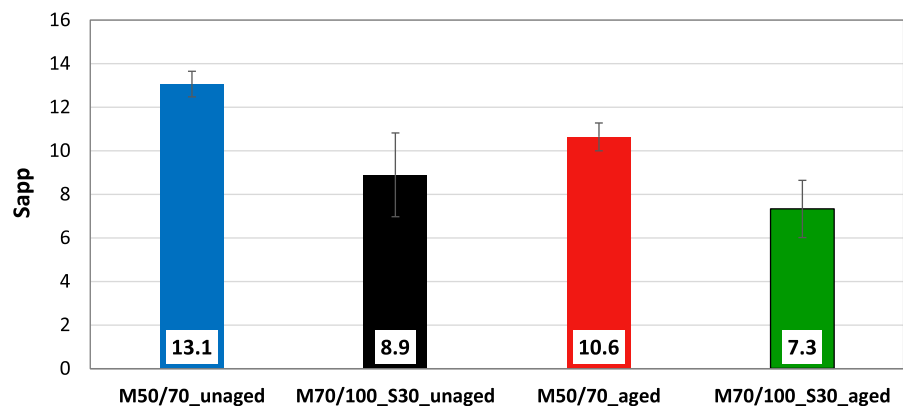


Fig. 6 D^R values (corresponding to the slope of the regression lines)

the D^R parameter. The results reveal higher D^R values in unaged conditions for both mixtures, in accordance with the expected trend reported in the literature [35, 63]. As for the comparison between the two mixtures, in both aging conditions, the reference asphalt mixture seems to be tougher than the bio-based one, and this result is consistent with the lower stiffness emerged from the complex modulus master curves (Fig. 2) and the lower pseudo-stiffness observed from the damage characteristic curves (Fig. 5).

In Fig. 7, the fatigue performance of the investigated mixtures is quantified through the apparent damage capacity index or S_{app} parameter (calculated for a climate PG 58–10 typical of central Italy [64]), which combines the effects of stiffness, damage characteristics and toughness. As can be observed, given the same aging condition, a slightly lower S_{app}

Fig. 7 S_{app} values



value is observed for the mixture containing lignin with respect to the conventional asphalt mixture. These results are probably due to the higher stiffness of the mixture containing lignin as compared to the reference mixture in both aging conditions (see Fig. 2). Moreover, as expected, both mixtures show a reduction of the S_{app} parameter after long-term aging, as a result of binder oxidation, stiffening and other phenomena that occur during aging [35, 65, 66].

It is also worth noting that significant efforts were necessary to obtain at least three valid tests for the mixture containing lignin, especially after long-term aging, as denoted by the lower R^2 values in Fig. 6 and larger standard deviations in Fig. 7. This may be attributable to the adopted testing framework, which may not be entirely suitable for such materials, or other reasons that may be related to the characteristics of the test specimens (e.g., reduced representativeness due to the small geometry adopted). In fact, the criterion based on the allowable maximum aggregate size for choosing the diameter of the specimens may not be applicable for such mixtures, which could be characterised by a local heterogeneity due to the inhomogeneous dispersion of lignin in the binder. Therefore, further investigations on 100 mm diameter specimens or 38 mm diameter specimens with a smaller NMAS (< 16 mm) are strongly encouraged in the future.

4.3 Linking the viscoelastic properties of asphalt binders and asphalt mixtures

In order to verify the consistency between the results of this study and previous findings obtained at the binder level on the same materials, the outcomes of the

complex modulus tests conducted with the AMPT were compared with the results of frequency sweep tests carried out with a dynamic shear rheometer (DSR) in [36].

In that study, Gaudenzi et al. evaluated the effect of the presence of lignin in a large frequency and temperature domain (Fig. 8a, b), finding a global stiffening effect in unaged conditions, despite both binders (the lignin-based one and the conventional 50/70 bitumen) were characterised by the same consistency (i.e., pen grade). The same stiffening effect is confirmed at mixture scale, as demonstrated by an increase in the storage modulus (E_1) values (Fig. 2a), which is particularly evident in the low frequency (high temperature) region. Moreover, the increase of the elastic response due to lignin, highlighted at the mixture level in Sect. 4.1, is also consistent with the phase angle master curve of the binder, whose shape is similar to a modified binder and thus denotes substantial differences with respect to the reference bitumen. In particular, the trend shows a decrease of the phase angle as the frequency decreases or temperature increases, entailing the progressive predominancy of the elastic response (Fig. 8b). This behaviour could be mainly attributable to the presence of lignin particles, which give a kind of filler effect, as already observed at the mastic level for some types of filler [67]. In fact, analogously to the case of fillers, the lignin particles dominate the binder behaviour in the low frequency/high temperature region, leading to a horizontal asymptote (Fig. 8a). This consideration on the filler effect provided by lignin is confirmed by the

similar complex modulus values observed at low reduced frequencies for the unaged and long-term aged bio-binder in Fig. 8a (which suggests that the behaviour at such frequencies is independent of the aging level of the binder, contrarily to the 50/70 bitumen).

In general, after long-term aging, an increase in complex modulus was found both at binder and mixture levels (as expected). Specifically, a lower aging susceptibility emerged for the bio-based binder containing lignin, which is perfectly consistent with what found at mixture scale (Table 3). Indeed, significant reductions in the differences between unaged and long-term aged conditions emerged, so that the master curves related to the lignin-based material are very close (almost overlapped) both at the binder and mixture levels. This behaviour can be attributable to the well-recognised antioxidant properties of lignin [21, 68, 69].

4.4 Linking the fatigue behaviour of asphalt mixtures according to S-VECD approach and conventional approach

Given the promising consistency between the viscoelastic properties of the binders and the mixtures, the comparison in terms of mixture fatigue behaviour based on the S-VECD approach and the conventional Indirect Tensile Fatigue Test (ITFT) is also presented. The ITFT data derive from a comprehensive mechanical characterization previously carried out on the same materials [26]. It is worth recalling that the

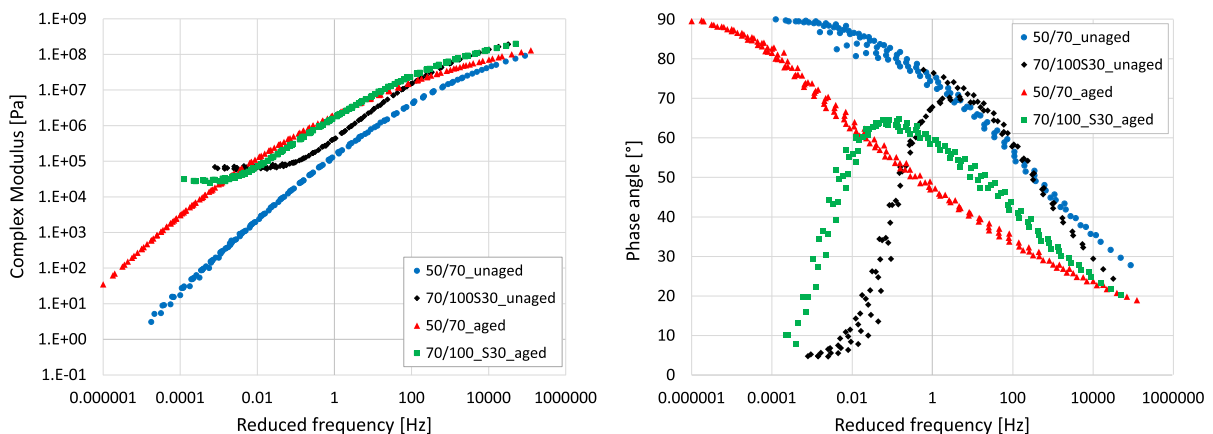


Fig. 8 Rheological properties of the asphalt binders studied: **a** complex modulus master curves and **b** phase angle master curves at 34 °C

mixtures involved in these two experimental investigations were characterised by the same aggregate gradation and binder content but different geometry and air voids, in accordance with the corresponding standards and/or specifications.

Figure 9 depicts the fatigue response of the lignin-based asphalt mixture and the reference mixture deriving from ITFT carried out at 20 °C, both in unaged and long-term aged conditions. In particular, the initial strain ε_0 is plotted as a function of the number of cycles at failure N_f . Moreover, the fatigue law and ε_6 parameter, corresponding to the strain level calculated at 10^6 cycles, are also provided in the figure. In unaged conditions, a shift of the fatigue curve of the lignin-based mixture towards the leftmost side of the graph is observed, together with a reduced ε_6 parameter, suggesting a penalization of the fatigue response. Even though these results greatly depend on the stress and strain conditions considered in the ITFT, the same result is observed also in terms of S_{app} parameter (S-VECD approach), which is based on intrinsic properties of the material (i.e., damage characteristic curve and D^R). Moreover, as expected, the aged reference mixture shows a reduced fatigue life as compared to the unaged conditions, and this is supported by both testing methods (S-VECD approach and ITFT). As for the lignin-based mixture M70/100_S30, according to the ITFT results, the mixture may be less vulnerable to the applied strain after aging, and a lower slope of the fatigue curve is observed as compared to the unaged mixture [26]. In terms of ε_6 parameter, the lignin-based mixture shows comparable fatigue response between the two aging conditions contrarily to the reference mixture characterized by a penalized performance in aged state, thus confirming its lower aging

susceptibility attributable to the presence of lignin. On the contrary, the results deriving from the S-VECD analysis showed a similar reduction of the S_{app} parameter for both mixtures after aging, indicating a penalisation of the fatigue resistance with respect to the corresponding unaged conditions, which is a typical effect of aging. However, it is worth noting that, as already mentioned in Sect. 4.2, the application of the S-VECD framework on lignin-based asphalt mixtures should be further investigated to confirm the reliability of the D^R and S_{app} parameters (Figs. 6 and 7) for these materials. In addition, the small geometry of the test specimens and/or the allowable maximum aggregate size in the S-VECD tests may have reduced the representativeness of the specimens, thus leading to a greater dispersion of the results.

5 Conclusions

The objective of this study was to compare a lignin-based mixture and a conventional asphalt mixture, particularly in terms of stiffness and fatigue properties. The bio-asphalt mixture was produced by using a plain bitumen (70/100 pen grade) partially replaced with 30% of lignin, thus resulting in a consistency similar to the 50/70 pen grade bitumen used to produce the conventional mixture. The mixtures were characterized by the same aggregate gradation but different binder content, as a result of a previous volumetric optimisation. The inclusion of lignin ultimately resulted in 15% bitumen saving. The mixtures were produced in the laboratory and tested in unaged and long-term aged conditions. The analysis was conducted by applying the S-VECD testing approach, which includes complex modulus and cyclic fatigue tests.

Despite the binders were characterised by a similar consistency (same pen. grade), the lignin-based mixture showed higher complex modulus and lower phase angle, denoting a stiffening effect and a more elastic behaviour attributable to the presence of lignin. The variation of the viscoelastic properties caused by long-term aging was lower for the mixture containing lignin as compared to the reference asphalt mixture, denoting its lower aging susceptibility. This finding is probably due to lignin antioxidant properties and/or the lower bitumen content in the bio-based mixture. In this

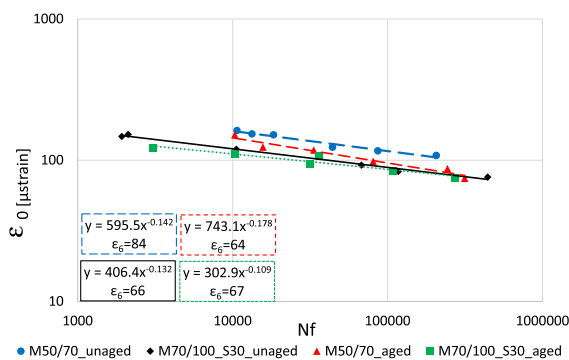


Fig. 9 Fatigue curves from ITFT and ε_6 parameter



regard, this study corroborates previous findings obtained at the binder level on the same materials.

This stiffening effect probably resulted in an embrittlement of the mixture containing lignin, which revealed slightly penalised fatigue behaviour in both aging conditions with respect to the reference asphalt mixture. The outcomes obtained in unaged conditions confirm previous findings deriving from conventional indirect tensile fatigue tests. On the contrary, the lower aging susceptibility was not fully confirmed by the S-VECD fatigue tests.

Finally, it is worth noting that significant efforts were necessary to obtain at least three valid fatigue tests for the mixture containing lignin, especially after long-term aging. This may be attributable to the small geometry of the test specimens (38 mm diameter), combined with the presence of lignin, the maximum aggregate size and the variability attributable to the presence of RAP, which may have reduced the representativeness of the specimens and partly penalised the repeatability of the tests. Moreover, even the adopted testing framework, including the definition of the parameters D^R and S_{app} , may not be entirely suitable for such materials. To clarify these aspects, further investigations on 100 mm diameter specimens or 38 mm diameter specimens with a smaller nominal maximum aggregate size (< 16 mm) are strongly recommended. Moreover, it should be pointed out that the results of this investigation cannot be generalised to all kinds of lignin, but they are strictly related to the specific lignin considered.

Author contribution Conceptualization, FC (FC); methodology, FC (FC) and LPI; experimental investigation, EG; resources, XL; data analysis, FC (FC), LPI, EG; writing – original draft preparation, EG; writing – review and editing, FC (FC) and LPI; supervision, XL and FC (FC). All authors have read and agreed to the published version of the manuscript.

Funding Open access funding provided by Università Politecnica delle Marche within the CRUI-CARE Agreement.

Open Access This article is licensed under a Creative Commons Attribution 4.0 International License, which permits use, sharing, adaptation, distribution and reproduction in any medium or format, as long as you give appropriate credit to the original author(s) and the source, provide a link to the Creative Commons licence, and indicate if changes were made. The images or other third party material in this article are included in the article's Creative Commons licence, unless

indicated otherwise in a credit line to the material. If material is not included in the article's Creative Commons licence and your intended use is not permitted by statutory regulation or exceeds the permitted use, you will need to obtain permission directly from the copyright holder. To view a copy of this licence, visit <http://creativecommons.org/licenses/by/4.0/>.

References

1. Reza S, Oliveira HS, Machado JJM, Tavares JMRS (2021) Urban safety: an image-processing and deep-learning-based intelligent traffic management and control system. *Sensors* 21(22):7705
2. Ingrassia LP, Lu X, Ferrotti G, Canestrari F (2020) Chemical, morphological and rheological characterization of bitumen partially replaced with wood bio-oil: towards more sustainable materials in road pavements. *J. Traffic Transp. Eng.* 7(2):192–204. <https://doi.org/10.1016/j.jtte.2019.04.003>
3. Gaudenzi E, Canestrari F, Lu X, Cardone F (2021) Performance assessment of asphalt mixture produced with a bio-based binder. *Materials (Basel)* 14(4):1–13. <https://doi.org/10.3390/ma14040918>
4. Lv S, Liu J, Peng X, Jiang M (2021) 2021 Laboratory experiments of various bio-asphalt on rheological and microscopic properties. *J Clean Prod* 320:128770. <https://doi.org/10.1016/j.jclepro.2021.128770>
5. Elahi Z et al (2021) Waste cooking oil as a sustainable bio modifier for asphalt modification: a review. *Sustain* 13(20):1–27. <https://doi.org/10.3390/su132011506>
6. Gaudenzi E, Cardone F, Lu X, Canestrari F (2023) The use of lignin for sustainable asphalt pavements: a literature review. *Constr Build Mater* 362(2022):129773. <https://doi.org/10.1016/j.conbuildmat.2022.129773>
7. Ren S et al (2021) Multi-scale characterization of lignin modified bitumen using experimental and molecular dynamics simulation methods. *Constr Build Mater* 287:123058. <https://doi.org/10.1016/j.conbuildmat.2021.123058>
8. Gao J, Wang H, Liu C, Ge D, You Z, Yu M (2020) High-temperature rheological behavior and fatigue performance of lignin modified asphalt binder. *Constr Build Mater* 230:117063. <https://doi.org/10.1016/j.conbuildmat.2019.117063>
9. Sun D et al (2017) Evaluation of optimized bio-asphalt containing high content waste cooking oil residues. *Fuel* 202:529–540. <https://doi.org/10.1016/j.fuel.2017.04.069>
10. Pouget S, Loup F (2013) Thermo-mechanical behaviour of mixtures containing bio-binders. *Road Mater Pavement Des.* <https://doi.org/10.1080/14680629.2013.774758>
11. Hu D, Gu X, Wang G, Zhou Z, Sun L, Pei J (2022) Performance and mechanism of lignin and quercetin as bio-based anti-aging agents for asphalt binder: A combined experimental and ab initio study. *J Mol Liq* 359:119310. <https://doi.org/10.1016/j.molliq.2022.119310>
12. Zhang L, Zhang S, Hu X, Gholizadeh M (2021) Progress in application of the pyrolytic lignin from pyrolysis of biomass. *Chem Eng J* 419(2020):129560. <https://doi.org/10.1016/j.cej.2021.129560>



13. Zhang S, Xiao J, Wang G, Chen G (2020) Enzymatic hydrolysis of lignin by ligninolytic enzymes and analysis of the hydrolyzed lignin products. *Bioresour Technol* 304:122975. <https://doi.org/10.1016/j.biortech.2020.122975>
14. J. Besamusca, P. Landa, R. Zoetemeyer, R. Gosselink, and B. Lommers, The use of lignin as bio-binder in asphalt applications Abstract Several investigations have shown interest in the use of durable material for road constructions, including bio-based oil, The introduction of lignin in asphalt.
15. Watkins D, Nuruddin M, Hosur M, Tcherbi-Narteh A, Jeevani S (2015) Extraction and characterization of lignin from different biomass resources. *J Mater Res Technol* 4(1):26–32. <https://doi.org/10.1016/j.jmrt.2014.10.009>
16. Safaei F, Castorena C, Kim YR (2016) Linking asphalt binder fatigue to asphalt mixture fatigue performance using viscoelastic continuum damage modeling. *Mech Time-Dependent Mater* 20(3):299–323. <https://doi.org/10.1007/s11043-016-9304-1>
17. Canestrari F, Ingrassia LP (2020) A review of top-down cracking in asphalt pavements: causes models experimental tools and future challenges. *J. Traffic Transp. Eng.* 7(5):541–572. <https://doi.org/10.1016/j.jtte.2020.08.002>
18. Xu C et al (2021) Effect of lignin modifier on engineering performance of bituminous binder and mixture. *Polymers (Basel)*. <https://doi.org/10.3390/polym13071083>
19. Norgbey E et al (2020) Unravelling the efficient use of waste lignin as a bitumen modifier for sustainable roads. *Constr Build Mater* 230:116957. <https://doi.org/10.1016/j.conbuildmat.2019.116957>
20. Zhang R et al (2020) Lignin structure defines the properties of asphalt binder as a modifier. *Constr Build Mater* 310:125156. <https://doi.org/10.1016/j.conbuildmat.2021.125156>
21. Zhang RJY, Liu X, Apostolidis P, Gard W, van de Ven M, Erkens S (2019) Chemical and rheological evaluation of aged Lignin-modified Bitumen. *Materials (Basel)* 12(24):4126
22. Fakhri M, Norouzi MA (2022) Rheological and ageing properties of asphalt bio-binders containing lignin and waste engine oil. *Constr Build Mater*. <https://doi.org/10.1016/j.conbuildmat.2022.126364>
23. Xu G, Wang H, Zhu H (2017) Rheological properties and anti-aging performance of asphalt binder modified with wood lignin. *Constr Build Mater* 151:801–808. <https://doi.org/10.1016/j.conbuildmat.2017.06.151>
24. Arafat S, Kumar N, Wasiuddin NM, Owhe EO, Lynam JG (2019) Sustainable lignin to enhance asphalt binder oxidative aging properties and mix properties. *J Clean Prod* 217:456–468. <https://doi.org/10.1016/j.jclepro.2019.01.238>
25. Zhang Y et al (2020) Mechanical performance characterization of lignin-modified asphalt mixture. *Appl Sci*. <https://doi.org/10.3390/app10093324>
26. Gaudenzi E, Cardone F, Lu X, Canestrari F (2022) Performance assessment of asphalt mixtures produced with a bio-binder containing 30 % of lignin. *Mater Struct*. <https://doi.org/10.1617/s11527-022-02057-w>
27. Di Benedetto H, De La Roche C, Baaj H, Pronk A, Lundström R (2004) Fatigue of bituminous mixtures. *Mater Struct Constr* 37(267):202–216. <https://doi.org/10.1007/bf02481620>
28. Kutay ME, Lanotte M (2018) Viscoelastic continuum damage (VECD) models for cracking problems in asphalt mixtures. *Int J Pavement Eng* 19(3):231–242. <https://doi.org/10.1080/10298436.2017.1279492>
29. Rondón-Quintana HA, Reyes-Lizcano FA, Zafra-Mejía CA (2021) Fatigue in asphalt mixtures – a summary to understand the complexity of its mathematical modeling. *J Phys Conf Ser* 2118(1):012009. <https://doi.org/10.1088/1742-6596/2118/1/012009>
30. Underwood B, Baek C, Kim Y (2012) Simplified viscoelastic continuum damage model as platform for asphalt concrete fatigue analysis. *Transp Res Rec* 2296:36–45. <https://doi.org/10.3141/2296-04>
31. Wang YD, Underwood BS, Kim YR (2022) Development of a fatigue index parameter, Sapp, for asphalt mixes using viscoelastic continuum damage theory. *Int J Pavement Eng* 23(2):438–452. <https://doi.org/10.1080/10298436.2020.1751844>
32. Spadoni S, Ingrassia LP, Mariani E, Cardone F, Canestrari F (2022) Long-term performance assessment of a warm recycled motorway pavement. *Case Stud. Constr. Mater.* 17:e01451. <https://doi.org/10.1016/j.cscm.2022.e01451>
33. Sadek H, Sadeq M, Masad E, Al-Khalid H, Sirin O (2019) Probabilistic viscoelastic continuum damage analysis of fatigue life of warm-mix asphalt. *J Transp Eng Part B Pavements* 145(3):04019024. <https://doi.org/10.1061/jpeodx.0000128>
34. Spadoni S, Ingrassia LP, Mocelin D, Richard Kim Y, Canestrari F (2022) Comparison of asphalt mixtures containing polymeric compounds and polymer-modified bitumen based on the VECD theory. *Constr Build Mater* 349:128725. <https://doi.org/10.1016/j.conbuildmat.2022.128725>
35. Ingrassia LP, Canestrari F (2022) VECD analysis to investigate the performance of long-term aged bio-asphalt mixtures compared to conventional asphalt mixtures. *Road Mater Pavement Des* 23(12):2697–2712. <https://doi.org/10.1080/14680629.2021.1991839>
36. A. E. Gaudenzi, F. Cardone, X. Lu, and F. Canestrari, Chemical and rheological analysis of short and long-term aged bio- extended binders containing lignin. Submitted to the *J. Traffic Transp. Eng.* (English Edition).
37. Gaudenzi E, Canestrari F, Lu X, Cardone F (2023) Performance analysis of bio-based asphalt mixtures containing Lignin. *Eur Transport*. <https://doi.org/10.48295/ET.2023.91.1>
38. Schapery RA (1984) Correspondence principles and a generalized J integral for large deformation and fracture analysis of viscoelastic media. *Int J Fract* 25(3):195–223. <https://doi.org/10.1007/BF01140837>
39. Kim YR, Lee YC, Lee HJ (1995) Correspondence principle for characterization of asphalt concrete. *J Mater Civ Eng* 7(1):59–68. [https://doi.org/10.1061/\(asce\)0899-1561\(1995\)7:1\(59\)](https://doi.org/10.1061/(asce)0899-1561(1995)7:1(59))
40. Daniel YR, J. S, and Kim, (2002) Development of a simplified fatigue test and analysis procedure using a viscoelastic continuum damage model. *Asph. Paving Technol.* AAPT 71:619–650
41. Chehab GR, Kim YR, Schapery RA, Witczak MW, Bonquist R (2002) Time-temperature superposition principle for asphalt concrete with growing damage in tension state. *Asph. Paving Technol Assoc. Asph. Paving Technol. Tech. Sess.* 71:559–593



42. Schapery RA (1990) A theory of mechanical behavior of elastic media with growing damage and other changes in structure. *J Mech Phys Solids* 38(2):215–253. [https://doi.org/10.1016/0022-5096\(90\)90035-3](https://doi.org/10.1016/0022-5096(90)90035-3)
43. Park SW, Kim YR, Schapery RA (1996) A viscoelastic continuum damage model and its application to uniaxial behavior of asphalt concrete. *Mech Mater* 24(4):241–255. [https://doi.org/10.1016/S0167-6636\(96\)00042-7](https://doi.org/10.1016/S0167-6636(96)00042-7)
44. Underwood BS, Kim YR, Guddati MN (2010) Improved calculation method of damage parameter in viscoelastic continuum damage model. *Int J Pavement Eng* 11(6):459–476. <https://doi.org/10.1080/10298430903398088>
45. Wang Y, Richard Kim Y (2019) Development of a pseudo strain energy-based fatigue failure criterion for asphalt mixtures. *Int J Pavement Eng* 20(10):1182–1192. <https://doi.org/10.1080/10298436.2017.1394100>
46. Wang YD, Keshavarzi B, Kim YR (2018) Fatigue performance prediction of asphalt pavements with FlexPAVE. *Transp Res Record*. <https://doi.org/10.1177/0361198118756873>
47. C. Castorena, Y. R. Kim, S. Pape, and K. Lee, Development of small specimen geometry for asphalt mixture performance testing IDEA program final report NCHRP IDEA Project N-181, no. October 2018, 2017.
48. AASHTO TP 133 (2021): Standard method of test for determining the damage characteristic curve and failure criterion using the asphalt mixture performance tester (AMPT) cyclic fatigue test, pp 0–30
49. U.S. Department of Transportation-Federal Highway Administration. Office of Preconstruction, Construction, and Pavements. Cyclic fatigue index parameter (Sapp) for asphalt performance engineered mixture design, vol. TechBrief, 2019.
50. CSA_Capitolato Speciale d'Appalto. Norme tecniche ANAS. Pavimentazioni stradali/autostradali. Allegato D.
51. National Cooperative Highway Research Program. Mixing and compaction temperatures of asphalt binders in hot-mix asphalt. In Transportation Research Board; NCHRP: Washington, DC, USA, 2010; 648.
52. AASHTO R 30–02 (2019) Standard practice for mixture conditioning of hot mix asphalt, Am. Assoc. State Highw. Transp. Off. 2(2019):1–5.
53. AASHTO PP99 (2019) - Standard practice for preparation of small cylindrical performance test specimens using the Superpave gyratory compactor (SGC) or field cores.
54. EN 12697–6–2012 (2012) Bituminous mixtures - Test methods for hot mix asphalt - Part 6: Determination of bulk density of bituminous specimens.
55. AASHTO TP 132 (2019) Standard method of test for determining the dynamic modulus for asphalt mixtures using small specimens in the asphalt mixture performance Tester (AMPT).
56. Olard F, Di Benedetto H (2003) General '2S2P1D' model and relation between the linear viscoelastic behaviours of bituminous binders and mixes. *Road Mater Pavement Des* 4(2):185–224. <https://doi.org/10.1080/14680629.2003.9689946>
57. G. D. Airey and G. D. Airey, (2011) Road materials and pavement design use of black diagrams to identify inconsistencies in rheological data use of black diagrams to identify inconsistencies in rheological data, no. June 2013, pp 37–41
58. Zhu J, Ahmed A, Said S, Dinegdae Y, Lu X (2021) 2022 Experimental analysis and predictive modelling of linear viscoelastic response of asphalt mixture under dynamic shear loading. *Constr Build Mater* 3:127095. <https://doi.org/10.1016/j.conbuildmat.2022.127095>
59. Chehab R, G.R., Kim, Y.R., Schapery, R.A., Witczak, M.W., Bonaquist, (2022) Time-temperature superposition principle for asphalt concrete with growing damage in tension state. *J. Assoc. Asph. Paving Technol.* 71:559–593
60. Pan T (2012) A first-principles based chemophysical environment for studying lignins as an asphalt antioxidant. *Constr Build Mater* 36:654–664. <https://doi.org/10.1016/j.conbuildmat.2012.06.012>
61. C. Hobson (2017) Evaluation of lignin as an antioxidant in asphalt binders and bituminous mixtures, no. January, 2017, [Online]. Available: www.ntis.gov.
62. Babadopulos LFDA, Ferreira JLS, Soares JB, Nascimento LAHD, Castelo Branco VT (2016) Aging-effect incorporation into the fatigue-damage modeling of asphalt mixtures using the S-VECD model. *J Mater Civ Eng* 28(12):04016161
63. Baek C, Underwood B, Kim Y (2012) Effects of oxidative aging on asphalt mixture properties. *Transp Res Rec* 2296:77–85. <https://doi.org/10.3141/2296-08>
64. F. Giuliani, (2008) Definizione di una mappa nazionale di Performance Grade dei bitumi stradali, *STRADE&COSTRUZIONI*, pp 1–12
65. Yousefi Rad F, Elwardany MD, Castorena C, Kim YR (2017) Investigation of proper long-term laboratory aging temperature for performance testing of asphalt concrete. *Constr Build Mater*. <https://doi.org/10.1016/j.conbuildmat.2017.04.197>
66. Zhang R, Sias JE, Dave EV, Rahbar-Rastegar R (2019) Impact of aging on the viscoelastic properties and cracking behavior of asphalt mixtures. *Transp Res Rec* 2673(6):406–415. <https://doi.org/10.1177/0361198119846473>
67. Mazzoni G, Stimilli A, Cardone F, Canestrari F (2017) Fatigue, self-healing and thixotropy of bituminous mastics including aged modified bitumens and different filler contents. *Constr Build Mater* 131:496–502. <https://doi.org/10.1016/j.conbuildmat.2016.11.093>
68. Wu J, Liu Q, Wang C, Wu W, Han W (2021) Investigation of lignin as an alternative extender of bitumen for asphalt pavements. *J Clean Prod* 283:124663. <https://doi.org/10.1016/j.jclepro.2020.124663>
69. Zarei A, Zarei M, Janmohammadi O (2019) Evaluation of the effect of Lignin and glass fiber on the technical properties of asphalt mixtures. *Arab J Sci Eng* 44(5):4085–4094. <https://doi.org/10.1007/s13369-018-3273-4>

